

## EFFECT OF HYDROTHERMAL AGING OVER A COMMERCIAL DOC ON NO<sub>2</sub> PRODUCTION AND SUBSEQUENT SCR EFFICIENCY

Tae Joong Wang\*

Aftertreatment System Development Part, Doosan Infracore, 489 Injung-ro, Dong-gu, Incheon 22502, Korea

(Received 8 February 2018; Revised 23 April 2018; Accepted 26 April 2018)

**ABSTRACT**—In this study, the effect of hydrothermal aging over a commercial diesel oxidation catalyst (DOC) on deterioration in nitrogen dioxide (NO<sub>2</sub>) production activity has been experimentally investigated based on a micro-reactor DOC experiment. Through this experimental result, the NO<sub>2</sub> to nitrogen oxides (NO<sub>x</sub>) ratio at DOC outlet has been mathematically expressed as a function of DOC temperature according to various aging conditions. The current study reveals that the catalyst aging temperature is a more dominant factor than the aging duration in terms of the decrease in NO<sub>2</sub> production performance through DOC. The DOC sample hydrothermally aged for 25 h at 750 °C has displayed the lowest NO<sub>2</sub> to NO<sub>x</sub> ratio compared to the samples aged for 25 ~ 100 h at 650 °C. Also, in this study, the impact of hydrothermal aging of a DOC on the selective catalytic reduction (SCR) efficiency in a ‘DOC + SCR’ aftertreatment system was predicted by using transient SCR simulations. To validate the SCR simulation, this study has conducted a dynamometer test of a non-road heavy-duty diesel engine with employing a commercial ‘DOC + SCR’ system on the exhaust line. The current study has quantitatively estimated the effect of the variation in NO<sub>2</sub> to NO<sub>x</sub> ratio due to the hydrothermal aging of DOC on the NO<sub>x</sub> removal efficiency of SCR.

**KEY WORDS** : Diesel engine, Exhaust aftertreatment system, Diesel oxidation catalyst, Selective catalytic reduction, Hydrothermal aging

### NOMENCLATURE

$C_i$  : coefficients for curve fit, non-dimensional  
 $T$  : temperature, °C  
 $y$  : NO<sub>2</sub> to NO<sub>x</sub> ratio, %

### 1. INTRODUCTION

Diesel engines have an excellent reputation for their lower fuel consumption, higher reliability and longer durability compared to other types of internal combustion engines (Jääskeläinen and Khair, 2018). In recent years, the exhaust emissions legislations of diesel engines have been increasingly stringent over the world. The primarily regulated emissions species include carbon monoxide (CO), hydrocarbons (HCs), particulate matter (PM) and NO<sub>x</sub> (Majewski, 2018). To comply with the emissions legislations, there has been a considerable advancement in the exhaust aftertreatment technologies (Johnson and Joshi, 2017; Johnson, 2016; Jääskeläinen and Majewski, 2018).

There are various kinds of diesel aftertreatment technologies such as diesel oxidation catalyst (DOC), diesel particulate filter (DPF), partial oxidation catalyst (POC) and selective catalytic reduction (SCR). In general, to meet the recent strict requirements of diesel emissions

regulations, these aftertreatment technologies are required as a combination system along with the dedicated sensors, controllers and thermal management systems. In particular, the ammonia SCR technology requires an additional injection system of a reducing agent (Brijesh and Sreedhara, 2013; Choi and Foster, 2006; Dan and Lee, 2016; Hirata *et al.*, 2009; Ko *et al.*, 2012; Nova and Tronconi, 2014; Pfahl *et al.*, 2012).

Especially in a combined aftertreatment system composed of DOC plus SCR, DOC is positioned prior to SCR because DOC has a cooperative effect on the operation of SCR in terms of the production of NO<sub>2</sub> (Allansson *et al.*, 2000; Bai *et al.*, 2016). It is well known that the impact of NO<sub>2</sub> to NO<sub>x</sub> ratio on SCR efficiency differs from the kinds of catalysts as well as the operating conditions. In general, the rate of ammonia SCR reaction reaches its maximum when the ratio of NO<sub>2</sub> to NO<sub>x</sub> becomes 50 %. However, if NO<sub>2</sub> to NO<sub>x</sub> ratio becomes higher than 50 %, then the SCR efficiency is drastically reduced (Koebel *et al.*, 2001, 2002). On the other hand, it is reported that the highest NO<sub>x</sub> conversion appears at over 50 % of NO<sub>2</sub> to NO<sub>x</sub> ratio under abundant ammonia dosage conditions for a Fe-zeolite SCR catalyst (Devadas *et al.*, 2006). Therefore, in ‘DOC + SCR’ systems, keeping NO and NO<sub>2</sub> concentrations as the best ratio at DOC outlet is important to efficiently control the overall NO<sub>x</sub> emissions in the subsequent SCR.

\*Corresponding author. e-mail: taejoong.wang@doosan.com

During engine lifetime, catalysts performance degrades due to harsh exhaust conditions. It is known that the decline in activity of the catalyst is strongly impacted by hydrothermal aging due to catalyst agglomeration and change in washcoat morphology (Dhillon *et al.*, 2017; Dosda *et al.*, 2016; Xi *et al.*, 2013).

This study has investigated on how the hydrothermal aging of a commercial DOC has an impact to its NO<sub>2</sub> production performance. Thus, the change in NO<sub>2</sub> to NO<sub>x</sub> ratio at DOC outlet according to hydrothermal aging conditions has been experimentally evaluated based on a DOC micro-reactor test. Also, this study may contribute to the literature by providing a mathematical relation on the NO<sub>2</sub> to NO<sub>x</sub> ratio at DOC outlet as a function of DOC temperature according to various aging conditions.

Moreover, in this study, the impact of the hydrothermal aging of DOC on the SCR efficiency in a ‘DOC + SCR’ system over a non-road transient cycle (NRTC) was predicted by using the well-established SCR simulation technique (<https://www.dieselnr.com/standards/cycles/nrtc.php>; Wang *et al.*, 2011, 2017). For the validation of SCR simulations, the current study has conducted a dynamometer test of a heavy-duty diesel engine with employing a commercial ‘DOC + SCR’ aftertreatment system on the exhaust line. Also, the current SCR simulations have quantitatively estimated the effect of the variation in NO<sub>2</sub> to NO<sub>x</sub> ratio on the NO<sub>x</sub> removal efficiency of SCR which was positioned downstream of the DOC.

## 2. DOC MICRO-REACTOR EXPERIMENT

### 2.1. Experimental Setup

In this study, a DOC experiment was conducted on a micro-reactor rig bench to evaluate the hydrothermal aging effect on the NO<sub>2</sub> production activity. The catalyst system of the current commercial DOC is composed of Pt/Pd and Al<sub>2</sub>O<sub>3</sub>. For this experiment, a small-sized (diameter × length = 25.4 mm × 25.4 mm) core part was taken out from a monolithic DOC converter, whose specification was listed in Table 1.

For the current experiments, several DOC samples were prepared after the different hydrothermal aging under a furnace environment at 650 °C (for 25, 50, 75 and 100 h) and at 750 °C (for 25 h) with 10 % H<sub>2</sub>O. Here, the feed gas composition was 150 ppm NO, 1200 ppm HC, 1800 ppm CO, 4.5 % CO<sub>2</sub>, 13 % O<sub>2</sub>, 5 % H<sub>2</sub>O and N<sub>2</sub> balance. Also, the reactor space velocity (SV) was maintained to 50000 h<sup>-1</sup>. The space velocity indicates the total volumetric flow rate divided by the volume of DOC monolith at standard condition (i.e., 101.325 kPa and 15 °C). In this experiment, the target amount of H<sub>2</sub>O was supplied to balance gas (N<sub>2</sub>) by regulating the relative humidity of water vapor. A schematic diagram of the current DOC micro-reactor test setup is presented in Figure 1.

In this test, the measurement of NO concentration was

Table 1. Specification of a commercial DOC.

Parameter	Value
Diameter	266.7 mm
Length	101.6 mm
Volume	5.68 dm <sup>3</sup>
Cell density	62 cm <sup>-2</sup> (400 cps)
Substrate wall thickness	177.8 μm
Catalyst type	Pt/Pd/Al <sub>2</sub> O <sub>3</sub>

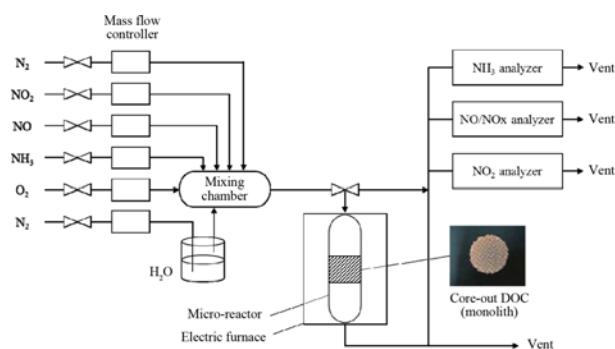


Figure 1. Micro-reactor experimental setup.

done by the online chemiluminescence NO-NO<sub>x</sub> analyzer (Thermo Electron Co., model 42H). Also, NO<sub>2</sub> was measured by the NO<sub>2</sub> analyzer equipped with electrochemical cell (Testo, model 350M), and NH<sub>3</sub> was measured by the NDIR-type NH<sub>3</sub> analyzer (Rosemount Analytical, model 880A).

### 2.2. Experimental Result and Curve-fit

Figure 2 displays the current experiment results which show the variation of NO<sub>2</sub> to NO<sub>x</sub> ratio versus temperature with the DOC samples prepared under different aging conditions. Also in Figure 2, the 5th order polynomial curve-fit results are provided together with the corresponding measurement data.

As shown in the figure, the fresh DOC sample shows the best performance in terms of NO<sub>2</sub> production activity. Hence, it delivers the highest NO<sub>2</sub> to NO<sub>x</sub> ratio over the entire temperature range tested in this study (i.e., 200 ~ 400 °C). For the fresh DOC catalyst, the maximum NO<sub>2</sub> to NO<sub>x</sub> ratio was measured to 54.0 % at 350 °C.

On the other hand, the hydrothermal aging for 25 h at 650 °C delivers a lower NO<sub>2</sub> to NO<sub>x</sub> ratio than the fresh sample at temperatures above 250 °C, while it shows a similar NO<sub>2</sub> production activity at 200 °C. Also, Figure 2 reveals that the NO<sub>2</sub> production performance becomes worse as the duration of the hydrothermal aging increases. In particular, the catalyst sample obtained after the hydrothermal aging for 25 h at 750 °C shows the lowest NO<sub>2</sub> to NO<sub>x</sub> ratio over the entire temperature range. This

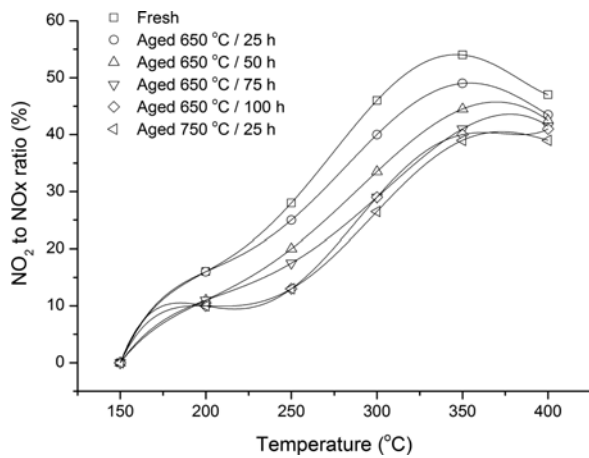


Figure 2. Measurement and curve-fit results of NO<sub>2</sub> to NOx ratio as a function of temperature with different DOC preparations. Feed gas composition: 150 ppm NO, 1200 ppm HC, 1800 ppm CO, 4.5 % CO<sub>2</sub>, 13 % O<sub>2</sub>, 5 % H<sub>2</sub>O and N<sub>2</sub> balance. Space velocity: 50000 h<sup>-1</sup>.

means that aging temperature is a more dominant factor than aging duration under the current test conditions.

Equation (1) describes the formulation of the 5th order polynomial curve fit that was adopted in this study. Also, Table 2 summarizes the coefficients of Equation (1). Note that seven digits under floating point were applied to the information given in Table 2.

$$y = -C_0 + C_1 \cdot T - C_2 \cdot T^2 + C_3 \cdot T^3 - C_4 \cdot T^4 + C_5 \cdot T^5 \quad (1)$$

In Figure 2, the measurement results of both '25 h at 750 °C' and '100 h at 650 °C' show almost the same NO<sub>2</sub> to NOx ratio at 150, 200, and 250 °C. But, the fitted curve of '25 h at 750 °C' estimates a slightly higher NO<sub>2</sub> to NOx ratio than that of '100 h at 650 °C' at this temperature range. This is because the curve fit below 250 °C is affected by other parts of data which were measured above 250 °C. Therefore, note that the results of Figure 2 include some curve-fit errors.

### 3. ENGINE DYNAMOMETER TEST

#### 3.1. Test Setup

In this study, an engine dynamometer test was conducted over a scheduled NRTC mode with employing a 'DOC + SCR' system on the exhaust line. Based on this test result, the NOx removal performance of heavy-duty diesel aftertreatment system was evaluated.

The diesel engine tested in this study has been widely used for various heavy-duty non-road applications such as excavators, wheel loaders and fork lift trucks. The specification of the diesel engine is summarized in Table 3. This engine has been developed and manufactured by Doosan Infracore Co., Ltd.

Figure 3 displays a schematic diagram of diesel engine and aftertreatment system including dynamometer test setup. The current exhaust aftertreatment system was composed of DOC and SCR, and the DOC was positioned prior to the SCR. Note that the type of SCR catalyst is based on a Cu-zeolite. Also, a urea dosing system and a mixer were located between the DOC and SCR. Table 4 summarizes the specification of SCR tested in this study.

In this test, the diesel engine was connected to a 460 kW AC dynamometer that is controlled by a STARS 1.6 control system. A test-cell computer controls the engine's speed and torque while recording the test data. The test cell has a full emissions bench with HORIBA MEXA-7100DEGR analyzer.

The diesel fuel used in this test is a ultra low sulfur diesel (ULSD) which contains 6.4 wt ppm sulfur and no oxygen. The supplier of this diesel fuel is GS Caltex Co. Ltd. The cetane number of this fuel is 55.4, and its density is 0.8232 g/cm<sup>3</sup> at 15 °C.

The NRTC test mode is a transient driving cycle for mobile non-road diesel engines developed by the United States (US) Environmental Protection Agency (EPA) in cooperation with the authorities in the European Union (EU). This test mode is used internationally for emission certification or type approval of non-road engines, and it has a total duration of 1238 s of transient driving schedule on an engine dynamometer (Emission Test Cycles;

Table 2. 5th order polynomial curve-fit information of Equation (1) for various hydrothermal aging conditions of a commercial diesel oxidation catalyst.

Coefficient	Fresh	Aged (650 °C / 25 h)	Aged (650 °C / 50 h)	Aged (650 °C / 75 h)	Aged (650 °C / 100 h)	Aged (750 °C / 25 h)
C <sub>0</sub>	1.3390000E+03	1.1935000E+03	5.2250000E+02	5.0150000E+02	1.9130000E+03	1.2910000E+03
C <sub>1</sub>	2.6559667E+01	2.3053167E+01	9.8158333E+00	8.9968333E+00	3.8062333E+01	2.5007667E+01
C <sub>2</sub>	2.0528333E-01	1.7300833E-01	7.1541667E-02	6.1725000E-02	2.9251667E-01	1.8650000E-01
C <sub>3</sub>	7.7366667E-04	6.3283333E-04	2.5300000E-04	2.0283333E-04	1.0876667E-03	6.7100000E-04
C <sub>4</sub>	1.4066667E-06	1.1166667E-06	4.2333333E-07	3.1000000E-07	1.9533333E-06	1.1600000E-06
C <sub>5</sub>	9.8666667E-10	7.6000000E-10	2.6666667E-10	1.7333333E-10	1.3600000E-09	7.7333333E-10

Table 3. Specification of a diesel engine.

Parameter	Value
Bore × Stroke	100 mm × 125 mm
Number of cylinders	6 (in-line)
Displacement	5.89 dm <sup>3</sup>
Fuel injection	Common-rail direct injection
Aspiration	Turbocharged/aftercooled
Rated power	141 kW @ 1900 rpm
Maximum torque	804 Nm @ 1400 rpm

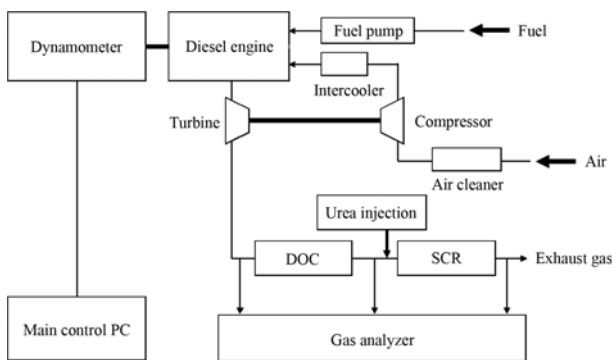


Figure 3. Engine dynamometer test setup with a commercial ‘DOC + SCR’ aftertreatment system.

Table 4. Specification of a commercial SCR.

Parameter	Value
Diameter	266.7 mm
Length	355.6 mm
Volume	19.87 dm <sup>3</sup>
Cell density	62 cm <sup>-2</sup> (400 cps)
Substrate wall thickness	177.8 μm
Catalyst type	Cu-zeolite

Nonroad Transient Cycle, 2018).

The NRTC test mode is composed of cold and hot start. Emission certification requires a weighted sum of cold and hot mode test. In this study, NRTC hot mode was selected as a duty cycle because it takes a major weighting portion (i.e., 95 % in US certification and 90 % in EU certification).

### 3.2. Test and Simulation Results for SCR NO<sub>x</sub> Conversion Performances

Engine bench test over a scheduled NRTC mode with hot start was conducted with measuring NO<sub>x</sub> emissions at both inlet and outlet of SCR catalyst. Also, engine performance

data and the injection quantity of diesel exhaust fluid (DEF) were measured at the same time. The DOC used in this engine dynamometer test was hydrothermally aged for 25 h at 750 °C with 10 % H<sub>2</sub>O.

Figure 4 displays the exhaust gas temperature measured at SCR inlet over NRTC hot mode. The exhaust temperature was 183.4 °C at the beginning of the cycle and its maximum value was 357.5 °C at 727 s. The cycle-averaged exhaust temperature was measured to 285.2 °C at SCR inlet in this NRTC hot test.

Figure 5 presents the space velocity profile that was obtained from a calculation of the measured exhaust volume flow rate at standard condition divided by the SCR volume specified in Table 4. The maximum space velocity was 32669 h<sup>-1</sup> at 339 s and the cycle-averaged value was measured to 18474 h<sup>-1</sup>.

Figure 6 shows the NO<sub>x</sub> concentration measured at SCR inlet over NRTC mode. In the current test, the maximum level of NO<sub>x</sub> emission was measured to 1004.6 ppm at 1158 s. It is worthwhile to note that several operating parameters and NO<sub>x</sub> emission at rated power of this engine are as follows; boosting pressure (i.e., pressure after

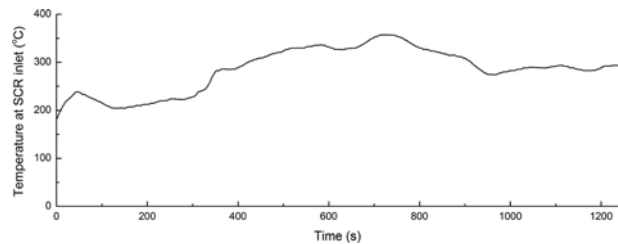


Figure 4. Measured exhaust temperature at SCR inlet over NRTC mode.

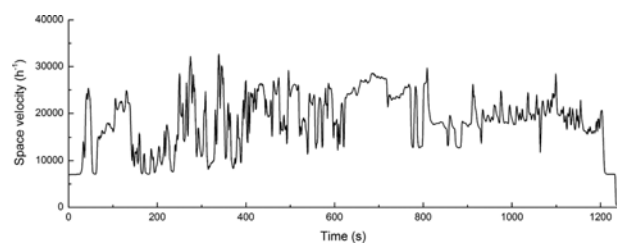


Figure 5. Measured space velocity at SCR inlet over NRTC mode.

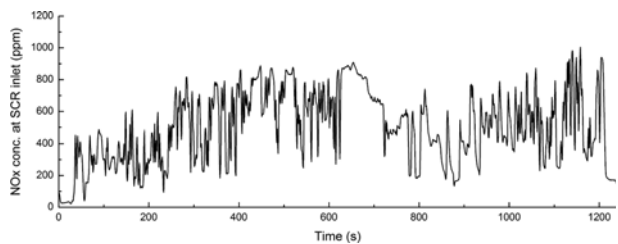


Figure 6. Measured NO<sub>x</sub> concentration at SCR inlet over NRTC mode.

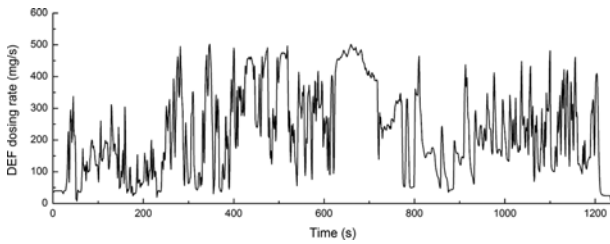


Figure 7. Measured DEF dosing rate at SCR inlet over NRTC mode.

compressor) 2.8 bar; common rail pressure 1800 bar; main injection timing 10 deg BTDC (before top dead center); pilot injection timing 16 BTDC; engine-out NO<sub>x</sub> concentration 1250 ppm.

Figure 7 illustrates the measured dosing rate of DEF. The maximum level of DEF dosing rate was measured to 502.1 mg/s at 347 s. In the current test, the threshold temperature of DEF injection was 180 °C at SCR inlet. Therefore, since the exhaust temperature was higher than 180 °C over the entire NRTC period, the DEF injection was not interrupted due to low temperature in this test.

Figures 8 and 9 show the validation results of the simulation data with the measurement data of NO<sub>x</sub> concentration at SCR outlet over the entire cycle period, in terms of both transient and cumulative basis. As shown in both figures, there is a good qualitative agreement between simulation and measurement. Note that the DOC used in this engine dynamometer test was hydrothermally aged for 25 h at 750 °C. Accordingly, the simulation results of

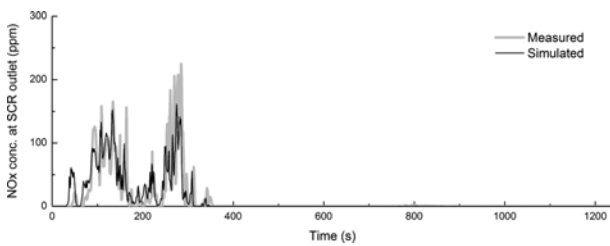


Figure 8. Comparison of the simulation result and the measurement result of NO<sub>x</sub> concentration at SCR outlet over NRTC mode.

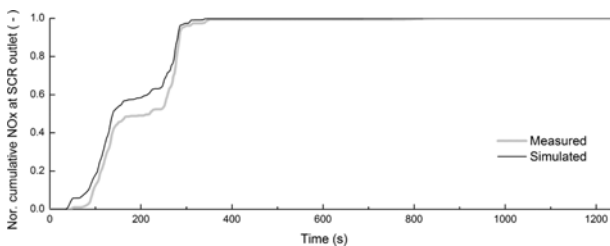


Figure 9. Comparison of the simulation result and the measurement result of the normalized cumulative NO<sub>x</sub> mass emission at SCR outlet over NRTC mode.

Figures 8 and 9 were obtained using Equation (1) with the coefficients listed in Table 2.

#### 4. EFFECT OF HYDROTHERMAL AGING OF DOC ON SUBSEQUENT SCR EFFICIENCY

On the basis of the well-validated SCR simulation technique (Wang *et al.*, 2011, 2017), this study has evaluated the effect of the hydrothermal aging of DOC on the NO<sub>x</sub> removal efficiency of SCR which was positioned downstream of the DOC.

Figure 10 displays the simulation results of the normalized cumulative NO<sub>x</sub> mass emission at SCR outlet over NRTC hot mode with the DOC samples that were hydrothermally aged under different conditions. As shown in the figure, the fresh DOC is expected to show the lowest emission of cumulative NO<sub>x</sub>. Also, the aging for 25 h at 650 °C would lead to a similar result to the fresh sample. On the other hand, the aging for 50 h at 650 °C would have a relatively large impact to the cycle-averaged SCR efficiency compared to the aging for 25 h at 650 °C. Also, the aging for 75 h at 650 °C would give a similar effect on the SCR efficiency with the aging for 50 h at 650 °C. Both DOC samples which were hydrothermally aged for 100 h at 650 °C and for 25 h at 750 °C would give the lowest SCR efficiency.

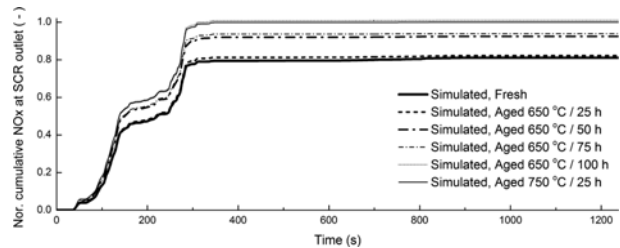


Figure 10. Simulation results of the normalized cumulative NO<sub>x</sub> mass emission at SCR outlet over NRTC mode with different DOCs.

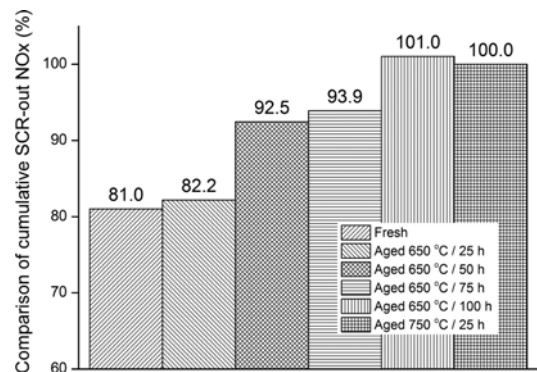


Figure 11. Relative comparison of cumulative SCR-out NO<sub>x</sub> of each DOC sample compared to that of the DOC aged for 25 h at 750 °C.

Figure 11 shows the relative comparison of cumulative SCR-out NO<sub>x</sub> of each DOC sample compared to that of the DOC aged for 25 h at 750 °C. It is expected that the hydrothermal aging of DOC for 25 h at 750 °C and for 100 h at 650 °C would increase 18 ~ 19 % level of cumulative tail-out NO<sub>x</sub> emission than that of the fresh DOC over NRTC hot mode. Also, the hydrothermal aging of DOC for 50 h at 650 °C and for 75 h at 650 °C would increase 11 ~ 12 % level of cumulative tail-out NO<sub>x</sub> emission than that of the fresh DOC over NRTC hot mode.

## 5. CONCLUSION

In this study, the deterioration in NO<sub>2</sub> production through a commercial DOC due to hydrothermal aging has been experimentally evaluated on the basis of a micro-reactor DOC test. Also, the impact of the hydrothermal aging of DOC on the SCR efficiency in a 'DOC + SCR' system over a non-road transient cycle was predicted by using the well-established SCR simulation technique. For the validation of SCR simulations, this study has conducted a dynamometer test of a heavy-duty diesel engine with employing a commercial 'DOC + SCR' aftertreatment system on the exhaust line.

A summary of the main results of this study is as follows:

- (1) The NO<sub>2</sub> production activity of DOC became worse as the duration of the hydrothermal aging increases.
- (2) Under the current test conditions, the catalyst aging temperature was a more dominant factor than the aging duration in terms of the deterioration in NO<sub>2</sub> production through DOC. The DOC sample obtained after the hydrothermal aging for 25 h at 750 °C showed the lowest NO<sub>2</sub> to NO<sub>x</sub> ratio compared to the samples aged for 25 ~ 100 h at 650 °C.
- (3) Both DOCs which were hydrothermally aged for 25 h at 750 °C and for 100 h at 650 °C showed almost the same NO<sub>2</sub> to NO<sub>x</sub> ratio at 150 ~ 250 °C.
- (4) Over a non-road transient cycle, it was expected that the hydrothermal aging of DOC for 25 h at 750 °C and for 100 h at 650 °C would increase 18 ~ 19 % level of cumulative tail-out NO<sub>x</sub> emission than that of the fresh DOC. Also, the hydrothermal aging of DOC for 50 h at 650 °C and for 75 h at 650 °C would increase 11 ~ 12 % level of cumulative tail-out NO<sub>x</sub> emission than that of the fresh DOC.

**ACKNOWLEDGEMENT**—The author would like to appreciate to the co-workers who have conducted the DOC micro-reactor experiment and the engine dynamometer test described in this study.

## REFERENCES

- Allansson, R., Cooper, B. J., Thoss, J. E., Uusimäki, A., Walker, A. P. and Warren, J. P. (2000). European experience of high mileage durability of continuously regenerating diesel particulate filter technology. *SAE Paper No.* 2000-01-0480.
- Bai, S., Tang, J., Wang, G. and Li, G. (2016). Soot loading estimation model and passive regeneration characteristics of DPF system for heavy-duty engine. *Applied Thermal Engineering*, **100**, 1292–1298.
- Brijesh, P. and Sreedhara, S. (2013). Exhaust emissions and its control methods in compression ignition engines: a review. *Int. J. Automotive Technology* **14**, **2**, 195–206.
- Choi, B. C. and Foster, D. E. (2006). Overview of the effect of catalyst formulation and exhaust gas compositions on soot oxidation in DPF. *J. Mechanical Science and Technology* **20**, **1**, 1–12.
- Dan, H. and Lee, J. (2016). Modeling and measurement of boiling point elevation during water vaporization from aqueous urea for SCR applications. *J. Mechanical Science and Technology* **30**, **3**, 1443–1448.
- Devadas, M., Kröcher, O., Elsener, M., Wokaun, A., Söger, N., Pfeifer, M., Demel, Y. and Mussmann, L. (2006). Influence of NO<sub>2</sub> on the selective catalytic reduction of NO with ammonia over Fe-ZSM5. *Applied Catalysis B: Environmental* **67**, **3-4**, 187–196.
- Dhillon, P. S., Harold, M. P., Wang, D., Kumar, A. and Joshi, S. (2017). Hydrothermal aging of Pt/Al<sub>2</sub>O<sub>3</sub> monolith: Washcoat morphology degradation effects studied using ammonia and propylene oxidation. *Catalysis Today*, DOI: <https://doi.org/10.1016/j.cattod.2017.12.023>.
- Dosda, S., Berthout, D., Mauviot, G. and Nogra, A. (2016). Modeling of a DOC SCR-F SCR exhaust line for design optimization taking into account performance degradation due to hydrothermal aging. *SAE Int. J. Fuels and Lubricants* **9**, **3**, 621–632.
- Emission Test Cycles; Nonroad Transient Cycle (2018). <https://www.dieselnet.com/standards/cycles/nrtc.php>
- Hirata, K., Masaki, N., Yano, M., Akagawa, H., Takada, K., Kusaka, J. and Mori, T. (2009). Development of an improved urea-selective catalytic reduction-diesel particulate filter system for heavy-duty commercial vehicles. *Int. J. Engine Research* **10**, **5**, 337–348.
- Jääskeläinen, H. and Khair, M. K. (2018). [https://www.dieselnet.com/tech/diesel\\_engines.php](https://www.dieselnet.com/tech/diesel_engines.php)
- Jääskeläinen, H. and Majewski, W. A. (2018). [https://www.dieselnet.com/tech/engine\\_heavy-duty\\_aftertreatment.php](https://www.dieselnet.com/tech/engine_heavy-duty_aftertreatment.php)
- Johnson, T. (2016). Vehicular emissions in review. *SAE Int. J. Engines* **9**, **2**, 1258–1275.
- Johnson, T. and Joshi, A. (2017). Review of vehicle engine efficiency and emissions. *SAE Paper No.* 2017-01-0907.
- Ko, A., Kim, J., Choi, K., Myung, C. L., Kwon, S., Kim, K., Cho, Y. J. and Park, S. (2012). Experimental study of particle emission characteristics of a heavy-duty diesel engine and effects of after-treatment systems: Selective catalytic reduction, diesel particulate filter, and diesel particulate and NO<sub>x</sub> reduction. *Proc. Institution of*

- Mechanical Engineers, Part D: J. Automobile Engineering* **226, 12**, 1689–1696.
- Koebel, M., Elsener, M. and Madia, G. (2001). Reaction pathways in the selective catalytic reduction process with NO and NO<sub>2</sub> at low temperatures. *Industrial & Engineering Chemistry Research* **40, 1**, 52–59.
- Koebel, M., Madia, G. and Elsener, M. (2002). Selective catalytic reduction of NO and NO<sub>2</sub> at low temperatures. *Catalysis Today* **73, 3-4**, 239–247.
- Majewski, W. A. (2018). [https://www.dieselnet.com/tech/em\\_i\\_intro.php](https://www.dieselnet.com/tech/em_i_intro.php)
- Nova, I. and Tronconi, E. (2014). *Urea-SCR Technology for deNO<sub>x</sub> after Treatment of Diesel Exhausts*. Springer. New York, USA.
- Pfahl, U., Schatz, A. and Konieczny, R. (2012). Advanced exhaust gas thermal management for lowest tailpipe emissions – Combining low emission engine and electrically heated catalyst. *SAE Paper No.* 2012-01-1090.
- Wang, T. J., Baek, S. W., Kwon, H. J., Kim, Y. J., Nam, I. S., Cha, M. S. and Yeo, G. K. (2011). Kinetic parameter estimation of a commercial Fe-zeolite SCR. *Industrial & Engineering Chemistry Research* **50, 5**, 2850–2864.
- Wang, T. J., Kim, D. S. and Ahn, T. S. (2017). Simulation study on improving the selective catalytic reduction efficiency by using the temperature rise in a non-road transient cycle. *Proc. Institution of Mechanical Engineers, Part D: J. Automobile Engineering* **231, 6**, 810–827.
- Xi, Y., Ottinger, N. A. and Liu, Z. G. (2013). Effect of hydrothermal aging on the catalytic performance and morphology of a vanadia SCR catalyst. *SAE Paper No.* 2013-01-1079.